

Evidence of fifth- and higher-order phonon scattering entropy of zone-center optical phonons


Xiaolong Yang^{1,2,*}, Tianli Feng^{3,*}, Ju Li^{4,†}, and Xiulin Ruan^{1,‡}

¹*School of Mechanical Engineering and the Birck Nanotechnology Center, Purdue University, West Lafayette, Indiana 47907-2088, USA*

²*College of Physics and Center of Quantum Materials and Devices, Chongqing University, Chongqing 401331, China*

³*Department of Mechanical Engineering, University of Utah, Salt Lake City, Utah 84112, USA*

⁴*Department of Nuclear Science and Engineering and Department of Materials Science and Engineering, Massachusetts Institute of Technology, Cambridge, Massachusetts 02139, USA*

 (Received 25 October 2021; revised 9 February 2022; accepted 15 March 2022; published 30 March 2022)

Authors of recent studies have established the significance of fourth-order anharmonicity in the linewidth of zone-center optical phonons, while it is unknown whether the fifth- and even higher-order phonon scattering is important. In this paper, we estimate the convergence of phonon scattering entropy with respect to perturbation orders. Using density functional perturbation theory, we calculate the three- and four-phonon linewidths for zone-center optical phonons in a series of zinc-blende III–V compounds including InP, c-GaN, BN, AlSb, GaP, InSb, AlAs, InAs, GaSb, and AIP. Our results show that, although the agreement between theory and experiment is greatly improved by incorporating four-phonon scattering, considerable discrepancies still exist, especially at high temperatures. We reveal that, on average, the phonon scattering entropy converges well at the eighth order, and the fifth- and higher-order phonon scattering entropy is about 37% of that of four-phonon scattering at Debye temperature and increases with temperature. With four-, five-, and higher-order phonon scattering included, the linewidth deviates largely from the linear scaling with temperature. In this paper, we provide evidence of the higher-than-fourth-order lattice anharmonicity in zone-center optical phonon linewidths as well as Raman and infrared spectra.

DOI: [10.1103/PhysRevB.105.115205](https://doi.org/10.1103/PhysRevB.105.115205)

I. INTRODUCTION

Zone-center optical phonon linewidth is a basic quantity in condensed matter, essential for a wide range of applications including material characterizations, infrared (IR) spectra, Raman spectra, and radiative heat transfer [1,2]. While three-phonon scattering had been considered the dominating mechanism for phonon linewidth [3–8], recently, fourth-order phonon anharmonicity has been predicted to have a significant or sometimes leading role [9–11]. First-principles predictions with four-phonon scattering have explained well the measured Raman or IR linewidths for a wide range of materials [11], and the method has been further extended to strongly anharmonic materials by including phonon frequency shift [12]. Although these works have facilitated increasing acceptance of the four-phonon scattering theory in spectroscopy techniques and radiative transport, a natural question is: What is the impact of the fifth- and even higher-order phonon scattering?

In this paper, we define and calculate the phonon *scattering entropy* of different orders of scattering for the zone-center optical phonons, using rigorous density functional theory (DFT) calculations for 10 zinc-blende III–V semiconductors including InP, c-GaN, BN, AlSb, GaP, InSb, AlAs, InAs, GaSb, and AIP. We find that, although four-phonon scattering can largely remedy the discrepancies between previous theory based on

three-phonon scattering and experiment, the fifth- and even higher-order phonon scattering can still be nonnegligible or even significant, especially above Debye temperature T_D .

II. METHODOLOGY

Phonon linewidth 2Γ is a Matthiessen sum of contributions from isotope (τ_{iso}^{-1}) [13,14], three-phonon ($\tau_{3,\lambda}^{-1}$) [15–17], four-phonon ($\tau_{4,\lambda}^{-1}$) [9,10,18], and higher-order phonon scattering rates [3,19]:

$$2\Gamma = \tau_{\text{iso}}^{-1} + \tau_{3,\lambda}^{-1} + \tau_{4,\lambda}^{-1} + \tau_{5,\lambda}^{-1} + \dots \quad (1)$$

The formalisms and calculations of τ_{iso}^{-1} , $\tau_{3,\lambda}^{-1}$, and $\tau_{4,\lambda}^{-1}$ are well established on the first-principles perturbation theory, and here, we follow the method as detailed in Ref. [11]. The second-, third-, and fourth-order interatomic force constants for calculating phonon frequencies and scattering rates were calculated from DFT within the local density approximation, as implemented in the Vienna *Ab initio* Simulation Package (VASP) [20,21]. The computational details as well as phonon dispersions of all materials studied are given in the Supplemental Material [22], including Refs. [23–37] therein. Direct evaluation of the five-phonon ($\tau_{5,\lambda}^{-1}$) and higher-order phonon scattering rates is currently not available. To estimate their significance, we define the scattering entropy of a phonon mode as

$$\begin{aligned} S &\equiv \frac{\hbar 2\Gamma}{T} = \frac{\hbar \tau_{\text{iso}}^{-1}}{T} + \frac{\hbar \tau_{3,\lambda}^{-1}}{T} + \frac{\hbar \tau_{4,\lambda}^{-1}}{T} + \frac{\hbar \tau_{5,\lambda}^{-1}}{T} + \dots \\ &\equiv S_2 + S_3 + S_4 + S_5 + \dots, \end{aligned} \quad (2)$$

*These authors contributed equally to this work.

†liju@mit.edu

‡ruan@purdue.edu

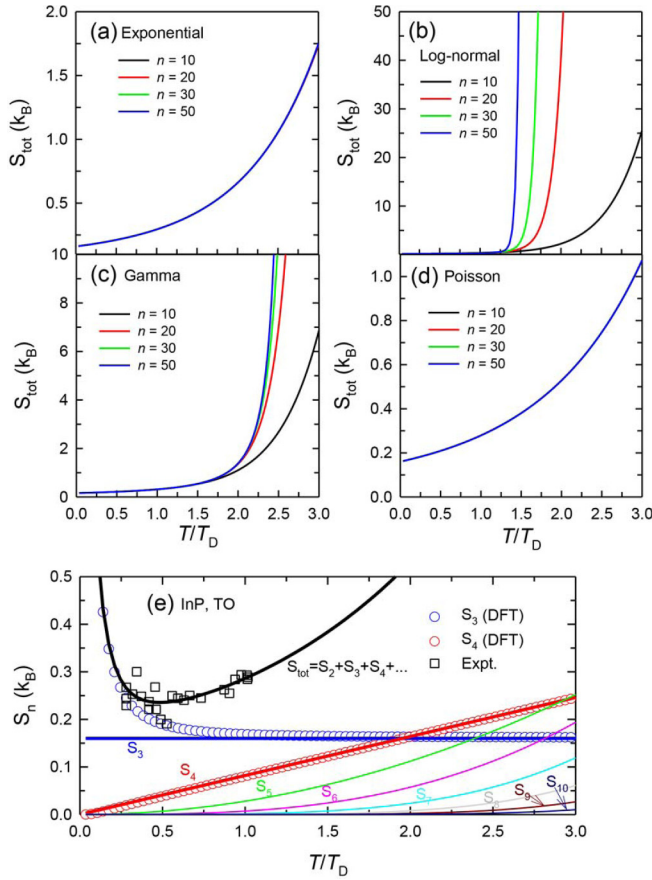


FIG. 1. (a) T -dependent entropy series summation of the transverse optical (TO) mode of InP with respect to n based on the exponential form, (b) log-normal function, (c) Gamma function, and (d) Poisson function. (e) Phonon scattering entropies of different order as a function of T for the TO mode of InP. The blue (red) circles represent the calculated S_3 (S_4), the black squares denote the experimental data from Ref. [38], and the solid curves represent the fitted results through Eq. (5). The total scattering entropy [$S_{\text{tot}} = (S_2 + S_3 + S_4)_{\text{DFT}} + S_5 + S_6 + \dots + S_{10}$] is provided for comparison with experiment.

considering that the quantity $\hbar 2\Gamma$ has a unit of energy and its temperature sensitivity has a unit of entropy. With this definition, S_2, S_3, S_4 , and S_5 are the phonon scattering entropies due to two- (isotope scattering), three-, four-, and five-phonon scattering, respectively. They count the multiplicities of phonon scattering reactions allowed by energy and momentum conservations. They should all have units of k_B , the Boltzmann constant, allowing easy numerical comparison of contributions at a particular temperature. They may themselves be T dependent: S_4, S_5 , and above grows strongly with increasing T .

Since $\tau_{3,\lambda}^{-1}$ increases approximately linearly and $\tau_{4,\lambda}^{-1}$ quadratically with T as shown before [9–11], and by analogy, $\tau_{5,\lambda}^{-1}$ increases cubically with T , $\hbar 2\Gamma$ can be asymptotically expanded as

$$\begin{aligned} \hbar 2\Gamma &= A + BT + CT^2 + DT^3 \dots \\ &= T(S_2 + S_3 + S_4 + S_5 + \dots), \end{aligned} \quad (3)$$

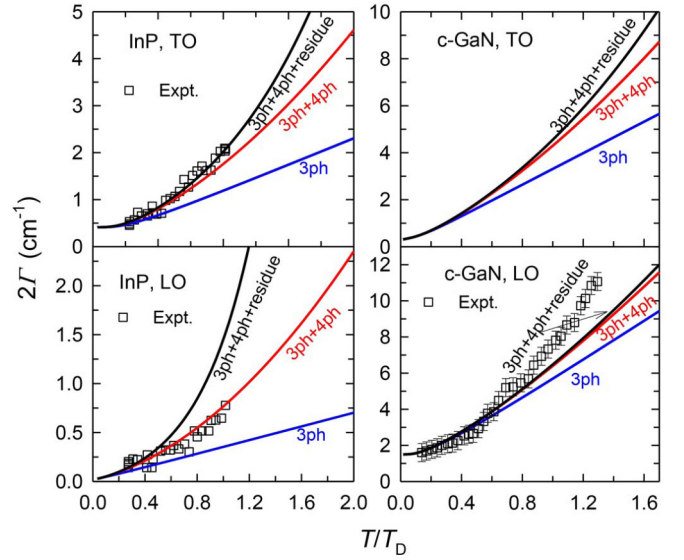


FIG. 2. T -dependent phonon linewidths 2Γ of the zone-center transverse optical (TO) and longitudinal optical (LO) phonons in InP and c-GaN. The solid red and blue curves represent our calculations with and without $\tau_{4,\lambda}^{-1}$; the solid black curves are the fitting results considering the higher-than-fourth-order phonon scattering terms; the squares denote experimental data for InP [38] and c-GaN [50]. Note that, for c-GaN, the T -independent background contribution arising from scattering by lattice defects is excluded from the original experimental data.

where the constant A accounts for the T -independent contribution from scattering with isotopes, impurities, and defects, BT for $\hbar\tau_{3,\lambda}^{-1}$, CT^2 for $\hbar\tau_{4,\lambda}^{-1}$, and DT^3 for $\hbar\tau_{5,\lambda}^{-1}$. Since different materials have different Debye temperatures, for cross-comparing between different materials, we introduce the dimensionless temperature scale $\tilde{T} \equiv T/T_D$ for normalization, and Eq. (3) can thus be rewritten as

$$\frac{\hbar 2\Gamma}{T} \equiv S = CT_D \left(\frac{\tilde{A}}{\tilde{T}} + \tilde{B} + \tilde{T} + \tilde{D}\tilde{T}^2 + \dots \right), \quad (4)$$

where CT_D is the four-phonon scattering entropy at $T = T_D$ ($\tilde{T} = 1$), which is used to normalize all the other scattering entropies, the dimensionless coefficients $\tilde{A} \equiv (A/T_D)/CT_D$, $\tilde{B} \equiv B/CT_D$, and $\tilde{D} \equiv DT_D/C$. If $\tilde{B} < 1$, then the three-phonon scattering is less important than the four-phonon scattering at $T = T_D$, and vice versa. If $\tilde{D} > 1$, the five-phonon scattering is more important than the four-phonon scattering at $T = T_D$, and vice versa.

Note that the higher the T , the more orders of scattering terms need to be included, and the absolute convergence of the linewidth will always be achieved. However, the higher-than-fourth orders are impractical to calculate directly at present. In this context, we attempt to establish an asymptotic form for estimating the higher-order phonon scattering entropy and for illustrating the convergence rate of the linewidth. In view of the variation law of phonon scattering of different order with T , we can easily deduce that the scattering entropy of different orders of phonon anharmonicity should have the form $k_B(T/T_D)^{n-3}f(n)$, with $f(n)$ representing the coefficient function associated with the scattering order n ($n \geq 3$). In

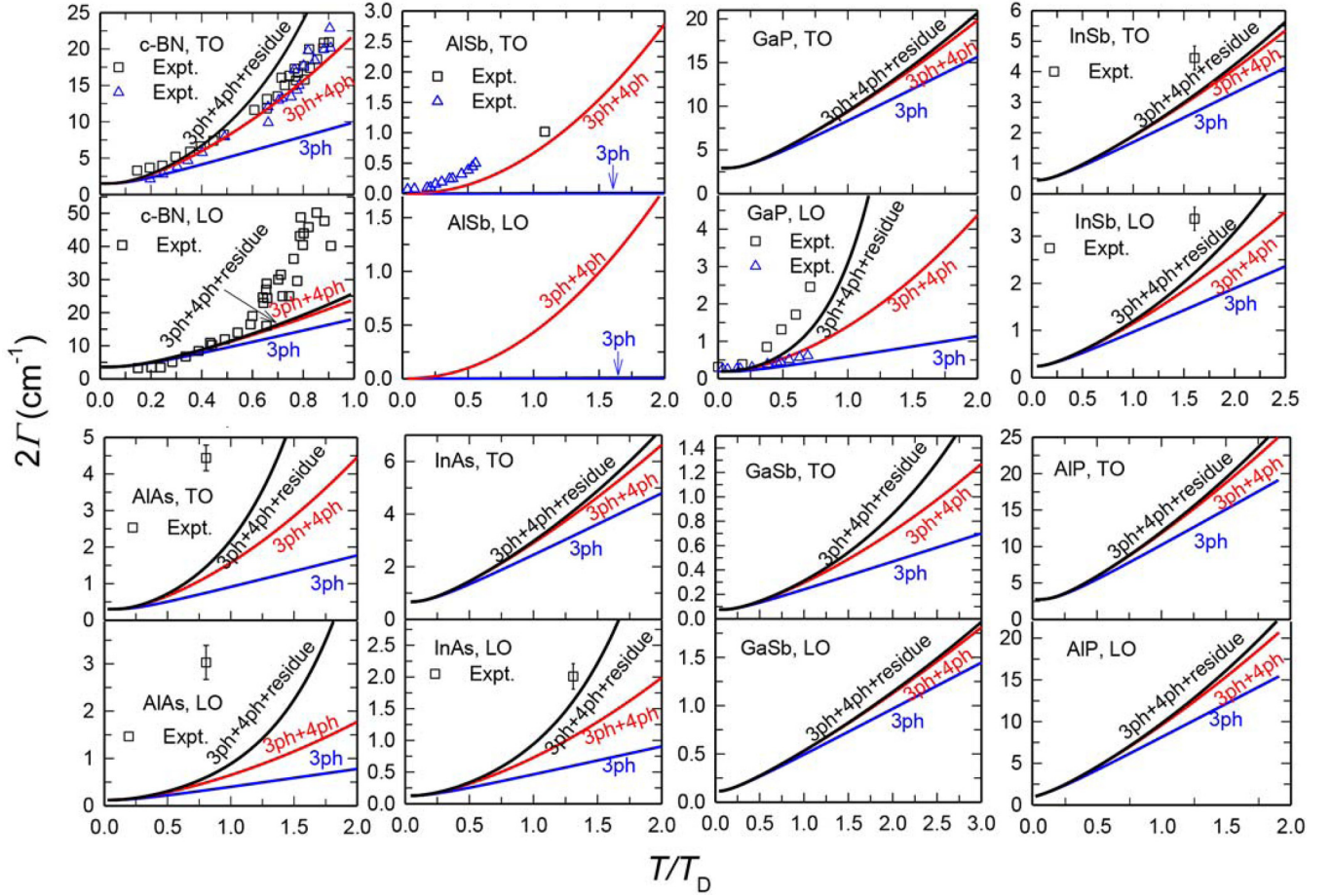


FIG. 3. Zone-center optical phonon linewidths 2Γ of the transverse optical (TO) and longitudinal optical (LO) phonons for group III-V zinc-blende compounds. The solid red and blue curves represent our calculated results with and without $\tau_{4,\lambda}^{-1}$, and the solid black curves are the fitting results considering the higher-than-fourth-order phonon scattering terms. Experimental data are taken from the following references: c-BN [39,40], AlSb [41,42], GaP [43,44], InSb [45], AlAs [45], and InAs [46,47].

principle, the scattering entropy must be absolutely convergent with n for any temperatures, thus $f(n)$ should be in the form of attenuation. By Occam's razor, the simplest analytical form is almost always the best. Here, we try to describe $f(n)$ with several different typical attenuation functions including the exponential form, log-normal function, Gamma function, and Poisson distribution. Once these functions allow the scattering entropy series summation to converge to a reasonable value for $T < T_{\text{melt}}$, where T_{melt} is the melting point, it makes sense for us to choose them as the coefficient function $f(n)$.

Taking the transverse optical (TO) mode of InP as an example, we apply these four functions to test the convergence rate of phonon scattering with increasing T . For the exponential form, $f(n) = \exp[-\alpha(T)n^2 + \beta(T)]$, and hence, the asymptotic form can be expressed as $S_n = k_B(T/T_D)^{n-3} \exp[-\alpha(T)n^2 + \beta(T)]$. By determining the parameters α and β from S_3 and S_4 at a given T , one can extrapolate the magnitude of higher-order phonon scattering and illustrate the convergence rate at different temperatures, especially above T_D . Figure 1(a) shows the entropy series summation with respect to n based on this fitting. It can be seen that, for $T/T_D < 3$, the convergence is achieved well at $n = 10$. For the log-normal function, $f(n) =$

$\frac{1}{(n-2)\alpha\sqrt{2\pi}} \exp\left\{-\frac{[\ln(n-2)-\beta]^2}{2\alpha^2}\right\}$. In Fig. 1(b), it appears that the entropy series summation obtained by log-normal function cannot give a convergent trend. For the Gamma function, $f(n) = \frac{(n-2)^{\alpha-1} \exp[-(n-2)/\beta]}{\Gamma(\alpha)\beta^\alpha}$, where α is a shape parameter, β is a scale parameter, and Γ is the usual generalized factorial $\Gamma(\alpha) = \int_0^\infty t^{\alpha-1} e^{-t} dt$. Note that n is set to 2 as the origin of the Gamma distribution since two-phonon scattering gives no contribution to the phonon anharmonicity. The entropy series summation obtained by the Gamma function is shown in Fig. 1(c). We can see that the convergence rate of scattering entropy is rather slow, and the convergence is not achieved even at $n = 50$. For the Poisson distribution, $f(n) = \frac{\alpha^{n-2} e^{-\alpha}}{(n-2)!}$, with the single parameter α being the expected rate of occurrences. Since the Poisson function has only one adjustable parameter, it cannot describe the scattering entropy of different order. To increase flexibility of the function, we introduce an additional parameter β to the original Poisson function to scale the amplitude of $f(n)$. Hence, the eventual form should be written as $f(n) = \beta \frac{\alpha^{n-2} e^{-\alpha}}{(n-2)!}$. Similarly, n is set to 2 as the origin of the Poisson distribution. It is observed in Fig. 1(d) that, at $T/T_D < 3$, the convergence of phonon scattering by fitting the Poisson distribution is well achieved at $n = 10$.

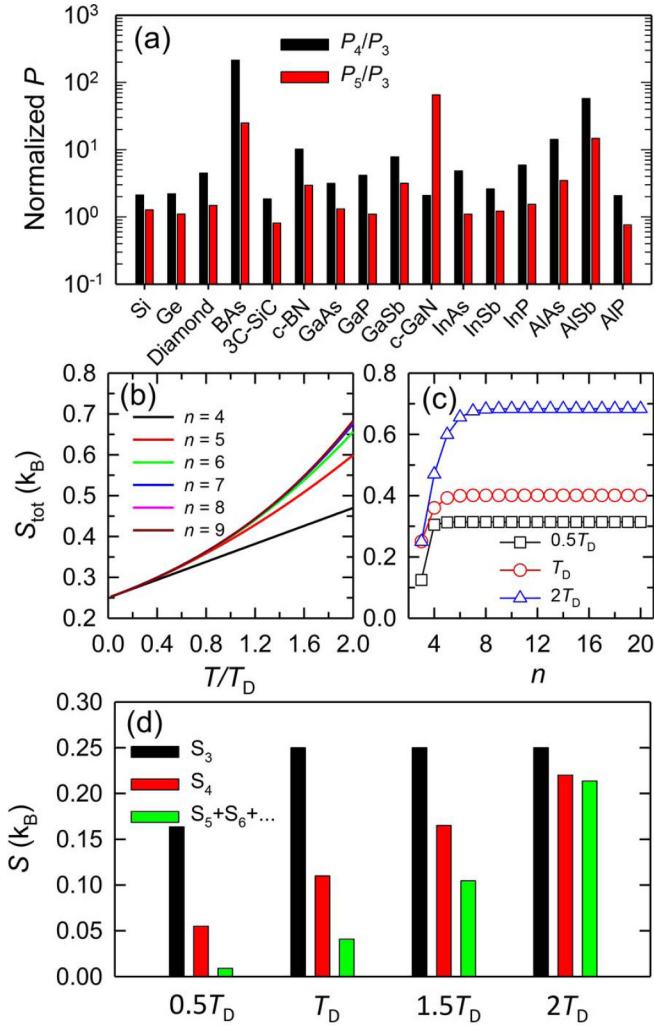


FIG. 4. (a) The normalized four- and five-phonon phase spaces of the zone-center transverse optical (TO) mode for materials studied. (b) The overall convergence speed of phonon scattering entropy with respect to the reduced temperature (T/T_D) when truncated to the different orders, and (c) with respect to the scattering order n at different temperatures. (d) The average scattering entropies S_3 , S_4 , and $S_5 + S_6 + \dots$ for materials studied at different temperatures.

From the above results, we conclude that, among these four functions, the exponential form and Poisson function are optimal for the convergence of phonon scattering. The exponential form, however, only works for the case where the scattering entropy decays monotonically with increasing n , whereas the Poisson function has the asymmetric shape and can thus reasonably reflect the nonmonotonic variation of scattering entropy, e.g., $S_3 < S_4 > S_5$. Given the realistic trend of scattering entropy with n , the Poisson distribution is preferred for describing $f(n)$. For further verifying the reliability of the Poisson function in terms of the convergence rate, we also show different orders of scattering entropy up to the tenth order in Fig. 1(e). It can be seen that the calculated S_4 (red circles) from the DFT is fitted well over the entire T range, whereas the calculated S_3 (blue circles) deviates from the fitted value below the T_D , due to the fact that $\tau_{3,\lambda}^{-1} \sim T$ is strictly satisfied only above T_D . Given that the higher-order

contributions are negligible below T_D , our proposed asymptotic form is valid in estimating higher-order entropy at high temperatures. It is clear from Fig. 1(e) that, in combination with the DFT calculations for S_2 , S_3 , and S_4 and the analytical fit for higher-order contributions, our estimated total scattering entropy [$S_{\text{tot}} = (S_2 + S_3 + S_4)_{\text{DFT}} + S_5 + S_6 + \dots + S_{10}$] (solid black line) can reasonably explain the experimental results (black squares), implying the validity of the Poisson function in estimating the convergence rate of phonon scattering.

Hence, in this paper, we propose the asymptotic form as

$$S_n = k_B \left(\frac{T}{T_D} \right)^{n-3} \beta \frac{\alpha^{n-2} e^{-\alpha}}{(n-2)!}, \quad (5)$$

which is the simplest analytical form of estimating the phonon anharmonicity ($n \geq 3$) to achieve absolute convergence following Occam's razor. Here, α and β are the fitting parameters related to the truncation order of scattering entropy and scattering strength, respectively, which are different for different phonon modes in different materials.

III. RESULTS AND DISCUSSION

The calculated zone-center phonon linewidths that include τ_{iso}^{-1} , $\tau_{3,\lambda}^{-1}$, and $\tau_{4,\lambda}^{-1}$ for the TO and longitudinal optical (LO) phonons in InP, c-GaN, c-BN, AlSb, GaP, InSb, AlAs, InAs, GaSb, and AlP are shown in Figs. 2–3 in comparison with available experimental data. For InP, we find that, with $\tau_{4,\lambda}^{-1}$ included, our calculated results are in good agreement with available experimental data [38], indicating that four-phonon scattering does account for the discrepancies between previous theoretical and experimental works. Remarkably, for other materials including c-GaN, c-BN, AlSb, GaP, InSb, AlAs, and InAs, our predictions of 2Γ , even after including four-phonon scattering, still deviate considerably from the experimental data in Refs. [39–47]. This implies that the fifth- and even higher-order phonon scatterings may become significant. For AlSb, the three-phonon contribution is nearly zero due to the large acoustic-optical (a-o) bandgap, and the four-phonon and higher-order processes dominate the linewidths in the entire T range. A similar case was also reported in BAs [11,48]. The large a-o phonon bandgap prevents two acoustic phonons from combining as an optical phonon due to the restriction of energy and momentum conservation as illustrated in Ref. [49]. For AlP and GaSb, which have no experimental data reported yet, our predictions provide a theoretical basis for the Raman measurements.

To assess the importance of fifth- and higher-order phonon scattering terms, we apply Eq. (5) to fit to S_3 and S_4 of the zone-center phonon linewidths of all the materials except AlSb, and the phonon scattering entropy of different order along with the fitting parameters is given in the Supplemental Material [22]. Note that, for AlSb, where the three-phonon contribution is nearly zero, our asymptotic form is not applicable anymore. The convergent linewidths obtained from the analytical fit are compared with the available experimental results in Figs. 2–3. For a certain mode of some of the materials studied, such as the TO mode of InP, LO mode of GaP, TO and LO modes of InSb, TO and LO modes of AlAs, LO mode of InAs, including the higher-order

TABLE I. Calculated characteristic scattering entropies $S_2 = A/T_D$, $S_3 = B$, and $S_4 = CT_D$ in terms of k_B , and the dimensionless coefficients \tilde{A} and \tilde{B} for materials examined in this paper. The relative contribution of four- to three-phonon scattering entropy at RT, $S_4(300\text{K})/S_3(300\text{K})$, is also given.

Materials	T_D (K)	S_2 (k_B)	S_3 (k_B)	S_4 (k_B)	\tilde{A}	\tilde{B}	RT- S_4/S_3
Si	645	0.039	0.34	0.076	0.51	4.39	10.59%
Ge	360	0.025	0.28	0.043	0.58	6.60	12.62%
Diamond	2280	0.026	0.12	0.091	0.28	1.32	9.93%
BAs	651	0.34	0.00023	0.12	2.76	0	52 173.91%
3C-SiC	1106	0.013	0.16	0.36	0.037	0.45	35.68%
c-BN	2025	0.030	0.19	0.24	0.13	0.65	9.73%
GaAs	313	0.021	0.23	0.13	0.16	1.74	51.86%
GaP	412	0.0044	0.69	0.096	0.046	7.19	8.89%
GaSb	240	0.0036	0.037	0.011	0.34	3.41	30.55%
c-GaN	584	0.0019	0.23	0.072	0.011	3.17	12.08%
InAs	229	0.032	0.41	0.082	0.39	5.04	24.70%
InSb	187	0.022	0.35	0.042	0.51	8.29	18.75%
InP	286	0.021	0.16	0.082	0.25	1.90	49.89%
AlAs	373	0.012	0.086	0.073	0.17	1.18	59.07%
AlSb	276	0.00031	0.00093	0.10	0.003	0.009	12 132.14%
AlP	525	0.092	0.71	0.12	0.74	5.70	8.50%
Average \bar{S}	–	0.043	0.25	0.11	–	–	–

scattering terms can considerably improve the agreement between the four-phonon theory-based calculations and experiments, showing the importance of higher-order effects. For both the LO modes of c-GaN and c-BN, our estimations show that the contribution of higher-order scattering terms is negligible, so we speculate that the difference between experiments [40,50] and our calculations may be due to the background scattering in the experiment, which is generally inevitable especially at higher temperatures. It should be noted that, in general, four-phonon scattering has a larger impact for optical phonons than for the heat-carrying acoustic phonons. Our previous studies [11,49] have shown that, for zone-center optical phonons, the four-phonon scattering is dominated by the recombination process $\lambda_1 + \lambda_2 \rightarrow \lambda_3 + \lambda_4$. The optical branches bunch together and allow the four modes λ_1 , λ_2 , λ_3 , and λ_4 to have similar energies, so they can easily satisfy the energy conservation rule for the recombination process. In contrast, the low-frequency acoustic phonons which carry heat rarely participate in the recombination process of the four-phonon scattering of optical phonons due to large energy differences. Therefore, it is understandable in certain materials, four-phonon scattering can significantly affect the linewidth of zone-center optical phonons, while not affecting much the thermal conductivity, e.g., in c-BN [51]. For the LO mode of InP and the TO mode of c-BN, the analytical fit reveals the significant contribution from higher-order terms at higher temperatures and overestimates the linewidth in varying degrees as compared with the experimental results. In addition to the limitations of the accuracy of our general model, this overestimation, at least in part, should be attributed to the T -induced phonon renormalization, which was not considered in this paper but has been demonstrated to considerably weaken the phonon scattering rates especially above T_D [52–54]. We also note that, with higher-order phonon scattering included, the linewidth deviates largely from the linear scaling with T , which offers an important theoretical basis

for experimentalists to study the Raman spectra at different temperatures.

To explore the significance of fifth-order phonon scattering, we further calculate the phase space P , which describe the probabilities of all the possible scattering events, of the zone-center TO phonon for three- (P_3), four- (P_4), and five-phonon (P_5) scattering in these materials, as given in the Supplemental Material [22]. Generally, the larger the phase space, the stronger the phonon scattering. For ease of comparison between different orders of scattering terms, we normalize P_4 and P_5 against P_3 , and results are shown in Fig. 4(a). As is seen in Fig. 4(a), P_5 is generally comparable with P_4 , especially for certain materials, e.g., c-GaN, P_5 is even an order of magnitude larger than P_4 , providing the evidence that the five-phonon scattering is indeed nonnegligible.

Table I lists the calculated detailed characteristic scattering entropies $S_2 = A/T_D$, $S_3 = B$, and $S_4 = CT_D$ in terms of k_B , and \tilde{A} and \tilde{B} for aforementioned compounds as well as some important materials studied in our recent work [11], including Si, Ge, diamond, BAs, and 3C-SiC. Also, for ease of appreciating the practical significance of the calculated numbers, the relative contribution of four- to three-phonon scattering entropy at room temperature (RT) $S_4(300\text{K})/S_3(300\text{K})$ is shown. The salient smallness of \tilde{T}_3 in some materials (BAs, AlSb, 3C-SiC, AlAs, and to a degree, InP) has to do with the peculiar phonon dispersion relation in these crystals, where the large a-o gap and the flatness of the optical bands make the satisfaction of three-phonon selection rules very difficult if not impossible. From the data, we have compiled the average entropies at their respective Debye temperatures, as shown in Table I. As is made explicit by the dimensionless expression in Eq. (4), when $\tilde{T} \ll \tilde{A}$, the linewidth is dominated by isotope/defect scattering. When $\tilde{T} > \tilde{B}$, four-phonon scattering is more important than three-phonon scattering. We also notice that the absolute magnitude of $S_4(T_D) = CT_D$ varies

TABLE II. Calculated phonon linewidth (in units of cm^{-1}) of the zone-center TO mode for materials studied in this paper as compared with the experimental values at around $T = T_D$.

Materials	T (K)	2Γ (exp) (cm^{-1})	2Γ ($\tau_{3,\lambda}^{-1}$) (cm^{-1})	2Γ ($\tau_{3,\lambda}^{-1} + \tau_{4,\lambda}^{-1}$) (cm^{-1})	2Γ [$\tau_{3,\lambda}^{-1} + \tau_{4,\lambda}^{-1} + (0.4\tau_{4,\lambda}^{-1})$] (cm^{-1})
Si	686	7.50 [55]	5.13	7.47	8.34
Ge	337	2.93 [56]	2.50	2.84	2.97
Diamond	1037	4.97 [57]	3.48	4.51	4.89
BAs	485	0.98 [11]	0.000017	0.97	1.33
InP	286	2.073 [38]	1.21	1.79	2.00
InSb	300	4.45 ± 0.39 [45]	2.66	3.16	3.35
c-BN	1826	20.96 [39]	8.98	18.79	22.42
AlAs	373	4.44 ± 0.35 [45]	0.91	1.56	1.80
AlSb	276	1.02 [42]	0.0021	0.80	1.10
GaAs	313	2.32 [38]	1.79	2.29	2.48
Average 2Γ	–	5.16	2.67	4.42	5.07

quite a lot, ranging from $0.011k_B$ in GaSb to $0.36k_B$ in 3C-SiC, implying that the four-phonon scattering strength is strongly correlated to the inherent phononic structure of the material such as the a-o gap, phonon bunching, and the flatness of the optical bands. On average, \bar{S}_4 ($0.11k_B$) is comparable with \bar{S}_3 ($0.25k_B$).

To provide insights on the overall convergence speed, we apply Eq. (5) to fit to \bar{S}_3 and \bar{S}_4 to extrapolate the total scattering entropy S_{tot} . Figure 4(b) shows the overall convergence speed of the total entropy below $T = 2T_D$ when truncated to the different orders. It is seen that the rate of convergence obviously depends on T : the higher the temperature, the slower the convergence rate. To look into the convergence rate more closely, Fig. 4(c) also shows the overall convergence speed with respect to the scattering order n for three certain temperatures. It is important to find that, within 0.01% error, the scattering entropy at $T = 0.5T_D$, T_D , and $2T_D$ converges well at the 6th, 8th, and 11th order, respectively. Physically significant is the fact that the Taylor expansion sum in Eq. (3) appears to have reasonable convergence rate on average but is not exceedingly rapid either, which one probably should have expected at the outset. More specifically, we find that the resulting higher-order scattering entropy $S_5 + S_6 + \dots$ is $0.041k_B$ at T_D , as much as $\sim 37\%$ of \bar{S}_4 . By carefully examining the T -dependent residual entropy between the experimental and the calculated scattering entropies $\Delta S \equiv S_{\text{exp}} - S_2 - S_3 - S_4$ for these materials, it appears that, on average, scattering processes higher than four-phonon scattering could still contribute considerably to the linewidth, as shown in Table II. On average, at $T = T_D$, the three-phonon scattering contribution to the linewidth is 2.67 cm^{-1} , and after including four-phonon scattering, the linewidth is 4.42 cm^{-1} , still lower than the experimental value of 5.16 cm^{-1} . When an additional $\sim 0.37\tau_{4,\lambda}^{-1}$ is included at $T = T_D$, the sum will approximately converge to the experiment value, demonstrating the robustness of our proposed asymptotic form in evaluating the high-order scattering terms. Thus, the total scattering entropies from all-order phonon scattering at $T = T_D$ should be about $S_2 + S_3 + S_4 + (S_5 + S_6 + S_7 + S_8) = 0.043k_B + 0.25k_B + 0.11k_B + (0.041k_B) = 0.44k_B$. The fact

that the average total scattering entropy is of the order of k_B is physically significant since it indicates universally that the zone-center optical phonon has a linewidth comparable with the average phonon energy at T_D . As is seen in Fig. 4(d), the residual entropy from higher-order terms increases rapidly with T : from our *ab initio* calculated data, we see that, at $T = 0.5T_D$, the residual contribution from the fifth- and higher-order scatterings is $< 2.86\%$, but at $T = 2T_D$, that is almost the same as \bar{S}_4 ($0.22k_B$).

IV. CONCLUSIONS

In summary, we have calculated the zone-center optical phonon linewidths of a series of technologically important III–V compound semiconductors by first principles. Including four-phonon scattering brings the predictions much closer to experimental data than the three-phonon theory. However, for many materials including c-GaN, c-BN, AlSb, GaP, InSb, AlAs, and InAs, the predictions, even after including four-phonon scattering, still deviate considerably from the experimental data. To examine the convergence of the phonon linewidth, we use the phonon scattering entropy concept, and an error-scale estimate for the previously untreated fifth- and higher-order phonon scattering entropies is provided for these materials on average. We find that, at T_D , on average, the convergence is well achieved at the eighth order, and the average entropy of fifth- and higher-order scattering is $\sim 37\%$ of that of four-phonon scattering. The total scattering entropy is of the order of k_B , which is physically significant since it indicates universally that the zone-center optical phonon has a linewidth comparable with the average phonon energy at T_D .

ACKNOWLEDGMENTS

X.Y. acknowledges the support from the China Scholarship Council (Grant No. 201706280325) and the Natural Science Foundation of China (Grant No. 12004254). Simulations have been performed at the Rosen Center of Advanced Computing at Purdue University.

- [1] M. Born and K. Huang, *Dynamical Theory of Crystal Lattices*, International Series of Monographs on Physics (Clarendon, Oxford, 1988), <https://books.google.com/books?id=5q9iRttaaDAC>.
- [2] Z. Zhang, *Nano/Microscale Heat Transfer* (McGraw-Hill, New York, 2007).
- [3] A. Debernardi, S. Baroni, and E. Molinari, *Phys. Rev. Lett.* **75**, 1819 (1995).
- [4] G. Lang, K. Karch, M. Schmitt, P. Pavone, A. P. Mayer, R. K. Wehner, and D. Strauch, *Phys. Rev. B* **59**, 6182 (1999).
- [5] A. Debernardi, *Phys. Rev. B* **57**, 12847 (1998).
- [6] A. Debernardi, C. Ulrich, K. Syassen, and M. Cardona, *Phys. Rev. B* **59**, 6774 (1999).
- [7] F. Bechstedt, P. Kckell, A. Zywietz, K. Karch, B. Adolph, K. Tenelsen, and J. Furthmüller, *Phys. Stat. Sol. (b)* **202**, 35 (1997).
- [8] X. Tang and B. Fultz, *Phys. Rev. B* **84**, 054303 (2011).
- [9] T. Feng and X. Ruan, *Phys. Rev. B* **93**, 045202 (2016).
- [10] T. Feng, L. Lindsay, and X. Ruan, *Phys. Rev. B* **96**, 161201(R) (2017).
- [11] X. Yang, T. Feng, J. S. Kang, Y. Hu, J. Li, and X. Ruan, *Phys. Rev. B* **101**, 161202(R) (2020).
- [12] Z. Tong, X. Yang, T. Feng, H. Bao, and X. Ruan, *Phys. Rev. B* **101**, 125416 (2020).
- [13] S.-i. Tamura, *Phys. Rev. B* **27**, 858 (1983).
- [14] S.-i. Tamura, *Phys. Rev. B* **30**, 849 (1984).
- [15] D. A. Broido, M. Malorny, G. Birner, N. Mingo, and D. A. Stewart, *Appl. Phys. Lett.* **91**, 231922 (2007).
- [16] L. Lindsay, D. A. Broido, and N. Mingo, *Phys. Rev. B* **82**, 115427 (2010).
- [17] L. Lindsay, D. A. Broido, and T. L. Reinecke, *Phys. Rev. Lett.* **109**, 095901 (2012).
- [18] T. Feng and X. Ruan, *Phys. Rev. B* **97**, 045202 (2018).
- [19] A. A. Maradudin and A. E. Fein, *Phys. Rev.* **128**, 2589 (1962).
- [20] G. Kresse and J. Hafner, *Phys. Rev. B* **47**, 558 (1993).
- [21] G. Kresse and J. Furthmüller, *Comput. Mater. Sci.* **6**, 15 (1996).
- [22] See Supplemental Material at <http://link.aps.org/supplemental/10.1103/PhysRevB.105.115205> for the computational details, phonon dispersions for all of materials examined in this paper, and convergence test of phonon scattering.
- [23] W. Li, J. Carrete, N. A. Katcho, and N. Mingo, *Comput. Phys. Commun.* **185**, 1747 (2014).
- [24] J. P. Perdew, K. Burke, and M. Ernzerhof, *Phys. Rev. Lett.* **77**, 3865 (1996).
- [25] O. Madelung, U. Rössler, and M. Schulz (eds.), in *Group IV Elements, IV-IV and III-V Compounds. Part a—Lattice Properties* (Springer, Berlin, Heidelberg, 2001), pp. 1–10.
- [26] H. Siegle, G. Kaczmarczyk, L. Filippidis, A. P. Litvinchuk, A. Hoffmann, and C. Thomsen, *Phys. Rev. B* **55**, 7000 (1997).
- [27] D. Strauch, in *New Data and Updates for IV-IV, III-V, II-VI and I-VII Compounds, their Mixed Crystals and Diluted Magnetic Semiconductors* (Springer, Berlin, Heidelberg, 2011), pp. 433–434.
- [28] O. Madelung, U. Rössler, and M. Schulz (eds.), in *Group IV Elements, IV-IV and III-V Compounds. Part b—Electronic, Transport, Optical and Other Properties* (Springer, Berlin, Heidelberg, 2002), pp. 1–5.
- [29] R. K. Ram and S. S. Kushwaha, *J. Phys. Soc. Jpn.* **54**, 617 (1985).
- [30] P. H. Borchers, G. F. Alfrey, A. D. B. Woods, and D. H. Saunderson, *J. Phys. C* **8**, 2022 (1975).
- [31] M. Yamaguchi, T. Yagi, T. Azuhata, T. Sota, K. Suzuki, S. Chichibu, and S. Nakamura, *J. Phys.: Condens. Matter* **9**, 241 (1997).
- [32] N. S. Orlova, *Phys. Stat. Sol. (b)* **103**, 115 (1981).
- [33] H. Bao and X. Ruan, *Int. J. Heat Mass Transf.* **53**, 1308 (2010).
- [34] M. I. Eremets, M. Gauthier, A. Polian, J. C. Chervin, J. M. Besson, G. A. Dubitskii, and Y. Y. Semenova, *Phys. Rev. B* **52**, 8854 (1995).
- [35] A. Togo, F. Oba, and I. Tanaka, *Phys. Rev. B* **78**, 134106 (2008).
- [36] K. Esfarjani, G. Chen, and H. T. Stokes, *Phys. Rev. B* **84**, 085204 (2011).
- [37] A. Kundu, N. Mingo, D. A. Broido, and D. A. Stewart, *Phys. Rev. B* **84**, 125426 (2011).
- [38] G. Irmer, M. Wenzel, and J. Monecke, *Phys. Stat. Sol. (b)* **195**, 85 (1996).
- [39] A. M. Zaitsev, A. A. Melnikov, V. B. Shipilo, and E. M. Shishonok, *Phys. Stat. Sol. (a)* **94**, K125 (1986).
- [40] H. Herchen and M. A. Cappelli, *Phys. Rev. B* **47**, 14193 (1993).
- [41] W. J. Turner and W. E. Reese, *Phys. Rev.* **127**, 126 (1962).
- [42] M. D. McCluskey, E. E. Haller, and P. Becla, *Phys. Rev. B* **65**, 045201 (2001).
- [43] I. V. Skryabinskii and Yu. I. Ukhanov, *Fiz. Tverd. Tela (Leningrad)* **15**, 1302 (1975) [*Sov. Phys.-Solid State* **16**, 1323 (1975)].
- [44] F. Vallee, *Phys. Rev. B* **49**, 2460 (1994).
- [45] D. Lockwood, G. Yu, and N. Rowell, *Solid State Commun.* **136**, 404 (2005).
- [46] R. W. Stimets and B. Lax, *Phys. Rev. B* **1**, 4720 (1970).
- [47] M. Hass and B. Hennis, *J. Phys. Chem. Solids* **23**, 1099 (1962).
- [48] L. Lindsay, D. A. Broido, and T. L. Reinecke, *Phys. Rev. Lett.* **111**, 025901 (2013).
- [49] X. Yang, T. Feng, J. Li, and X. Ruan, *Phys. Rev. B* **100**, 245203 (2019).
- [50] R. Cusco, N. Domenech-Amador, S. Novikov, C. T. Foxon, and L. Artus, *Phys. Rev. B* **92**, 075206 (2015).
- [51] K. Chen, B. Song, N. K. Ravichandran, Q. Zheng, X. Chen, H. Lee, H. Sun, S. Li, G. A. G. U. Gamage, F. Tian *et al.*, *Science* **367**, 555 (2020).
- [52] X. Gu, Z. Fan, H. Bao, and C. Y. Zhao, *Phys. Rev. B* **100**, 064306 (2019).
- [53] Y. Xia, K. Pal, J. He, V. Ozolins, and C. Wolverton, *Phys. Rev. Lett.* **124**, 065901 (2020).
- [54] Z. Han, X. Yang, S. E. Sullivan, T. Feng, L. Shi, W. Li, and X. Ruan, *Phys. Rev. Lett.* **128**, 045901 (2022).
- [55] M. Balkanski, R. F. Wallis, and E. Haro, *Phys. Rev. B* **28**, 1928 (1983).
- [56] J. Menendez and M. Cardona, *Phys. Rev. B* **29**, 2051 (1984).
- [57] W. Borer, S. Mitra, and K. Namjoshi, *Solid State Commun.* **9**, 1377 (1971).